Large Decadal Decline of the Arctic Multiyear Ice Cover

Josefino C. Comiso
Cryospheric Sciences Branch, NASA Goddard Space Flight Center

Address:
Cryospheric Sciences Branch, Code 614.1
NASA Goddard Space Flight Center
Greenbelt, MD, USA 20771

Email: Josefino.c.comiso@nasa.gov

Submitted to the Journal of Climate in February 2011

Abstract

The perennial ice area was drastically reduced to 38% of its climatological average in 2007 but recovered somewhat in 2008, 2009 and 2010 with the areas being 10%, 24%, and 11% higher than in 2007, respectively. However, the trends in the extent and area remain strongly negative at -12.2% and -13.5 %/decade, respectively. The thick component of the perennial ice, called multiyear ice, as detected by satellite data in the winters of 1979 to 2011 was studied and results reveal that the multiyear ice extent and area are declining at an even more rapid rate of -15.1% and -17.2 % per decade, respectively, with record low value in 2008 followed by higher values in 2009, 2010 and 2011. Such high rate in the decline of the thick component of the Arctic ice cover means a reduction in average ice thickness and an even more vulnerable perennial ice cover. The decline of the multiyear ice area from 2007 to 2008 was not as strong as that of the perennial ice area from 2006 to 2007 suggesting a strong role of second year ice melt in the latter. The sea ice cover is shown to be strongly correlated with surface temperature which is increasing at about three times global average in the Arctic but appears weakly correlated with the AO which controls the dynamics of the region. An 8 to 9-year cycle is apparent in the multiyear ice record which could explain in part the slight recovery in the last three years.

1. Introduction

The most visible change in the Arctic region has been the rapid decline of the perennial ice cover as previously reported by Comiso (2002). The perennial ice has been defined as the ice that survives the summer and represents the thick component of the sea ice cover. A drastic retreat of summer sea ice in the Beaufort Sea in 1998 was followed by record lows in the perennial ice cover in 2002 and in 2005. However, there was none more dramatic than in 2007 when the area of the perennial ice was reduced to about 37% of the climatological average value

and 28% the previous low value in 2005 (Comiso et al., 2008). Such drastic change in the perennial ice cover has been the subject of several studies (e.g., Perovich et al., 2009; Simmonds et al., 2008) and has been regarded as the event that could trigger an irreversible change in the Arctic sea ice cover (Lindsay et al., 2009; Serreze, 2009). The temperature of the upper layer of the Arctic Ocean is expected to have been increasing because of more solar heat absorbed by more extensive ice-free areas in the summer in recent years. The temperature may have already increased to a level which makes it difficult for sea ice to grow thick enough in winter and spring to be able to survive the summer melt period. The ice decline in 2007 has been attributed to the simultaneous occurrences of a number of phenomena including ice-albedo feedback (Zhang et al., 2008; Perovich et al., 2009), surface temperature (Steele et al., 2008; Shibata et al., 2010), winds and ice motion (Ogi et al., 2008; Kwok, 2008), increased cyclone activities (Simmonds et al., 2008) and an unusual cloud free condition (Kay et al., 2008; Schweiger et al., 2008). The observed trends in the ice cover is even more negative than those predicted by modeling studies (Stroeve et al., 2007) suggesting that the impact of greenhouse warming in the Arctic may be stronger than has been projected.

The dramatic decline of the perennial ice cover in 2007 was followed by a slight recovery for three consecutive years. Such recovery is intriguing and obviously needs to be better understood. Part of the recovery may be attributed to a global cooling that has been associated with the La Niña of 2008 the impact of which extended as far south as Antarctica where the sea ice extent in the region attained record high values in 2008. To gain insights into this phenomenon, we study the changes in the multiyear ice cover over the same 1978 to 2011 period as derived from passive microwave data during the winter months. Although the changes in the multiyear ice cover have been studied using active sensors like QuikScat (Ngheim et al., 2007; Kwok et al., 2009) the passive microwave data provide a more robust data set with a significantly longer record length

(32 years versus 12 years). Multiyear ice has been defined by WMO as ice that has survived at least two summer periods and is the thick component of the perennial ice cover which includes the relatively thinner second year ice cover. The difference in the signature of multiyear ice compared with seasonal ice has been reported previously (Vant et al., 1978) and has been confirmed using satellite data (e.g., Gloersen et al. 1992; Comiso, 2006). The study of the multiyear ice cover as described is important because it enables the assessment of changes and trends in the extent and area of this thick ice type over the more than three decades of continuous satellite observations. Analysis of the data could also provide the means to quantify the spatial changes in distribution and drift patterns of the old component of the perennial ice cover in autumn and winter. The interannual variability of the ice cover is examined in conjunction with observed changes in surface temperature, winds and sea level pressure.

2. Current State of the Arctic Sea Ice Cover

The Arctic sea ice cover is known to be highly seasonal with the ice extent changing from about 6 x 10^6 km^2 in the summer to about 15 x 10^6 km^2 in the winter (Comiso, 2010). The interannual changes are also known to be different for the different seasons with the interannual trends in winter being much more moderate than that in the summer. The pan-Arctic sea ice cover has undergone significant changes from November 1978 to December 2010 as depicted by the sea ice extent monthly anomalies presented in Figure 1a. The plot shows large yearly fluctuations of about 1 x 10^6 km^2 in the first 16 years but after the positive anomaly in 1996 the values went through a steady decline until 2007 when the dramatic decline in the ice cover at the end of summer was observed. It is apparent that the seasonal variability changed substantially since 2007 as well. Using linear regression, the trend in ice extent from 1978 to 2010 is estimated to be -4.0±0.2 % per decade while for the period 1996 to 2010, the trend is -8.3±0.6

%/decade. This indicates that since 1996, the Arctic sea ice cover has been declining at a rate that is more than twice the overall rate during the 1978 to 2010 period. Since 2007, the winter values were also close to previous values but falls down to extremely low summer minima. The lowest value in the anomaly plot is -2.4 x 10^6 km^2 which occurred in September 2007 while the September values in 2008, 2009 and 2010 were almost equally low.

Figure 1b shows how the seasonality of the Arctic sea ice cover has changed during the last three decades and the last few years. The three colored lines in the plots represent 10-year averages of daily data with the red line representing the first ten years of data (i.e., 979 to 1988), the blue representing the second ten years of data (i.e., 1989 to 1998), and the gold representing the third ten years of data (i.e., 1999 to 2008). The other lines represent data from individual years with the light gray line representing 2007, the darker gray line representing 2009 and the bold black line representing 2010. The plots indicate that the highest extent usually occurs around February or March while the lowest extents occur at the end of the summer melt period which usually happens during the month of September. In winter (e.g., January, February or March) the change in extent from the first to the second decade was almost zero while the change from the second to the third decade was slightly more and is around 0.6 x 10^6 km^2. In contrast, at the end of the summer (i.e., September), the changes are much more significant with the change from the first to the second decade being around 0.5 x 10^6 km^2 while that from the second to the third decade is around 1.2 x 10^6 km^2. The changes in the Arctic ice cover are thus more pronounced in the summer than in the winter period. The changes were even more drastic in the last four years as revealed by the individual plots in 2007, 2009 and 2010. The data for 2008 falls between those of 2007 and 2009 and was not shown to minimize overcrowding of the lines. Figure 1b also shows that the change from the first to the second decade was significant mainly in spring and summer while the change from the second to the third decade was significant in all

seasons. The largest interannual changes apparently occur at the end of the summer and during the summer minimum, and the values basically represents those of the perennial ice cover as described in Comiso (2002). Note that the ice extents for each day during the last week of December 2010 were significantly lower than those in previous years and were actually the record low values during the satellite era. Low values suggest a relatively warm winter that keeps the growth rate of ice (including thickness) relatively low. The persistence of such low values in winter would mean that a recovery for the perennial ice in 2011 is highly unlikely unless the surface temperatures in spring and summer are significantly colder than in recent years.

3. Multiyear Ice Concentration

Multiyear ice has been defined by the World Meteorological Organization as ice that has survived at least two summers. This ice type is the primary component of the perennial ice cover which also includes second year ice or ice that has survived only one summer. The passive microwave signature of multiyear ice is known to be significantly different from that of first year ice because of differences in salinity and therefore, dielectric properties (Vant et al., 1978). First year ice, which is also referred to as seasonal ice, is relatively saline because of the presence of brine entrapped during ice formation. On average, the surface salinity of first year ice is about 10 to 12 psu (Weeks and Ackley, 1986) while that of multiyear ice approaches 0 psu. Saline ice has a loss tangent (defined as the ratio of the imaginary and the real part of the dielectric constant) that is relatively high making it opaque to radiation while multiyear ice has a loss tangent that is low because of its low salinity making the material transparent to radiation and vulnerable to scattering effects. The net effect is a relatively high emissivity for first year ice and low emissivity for multiyear ice (Vant et al., 1978; Eppler et al., 1992). However, although the effective emissivity of first year ice is relatively well defined, the emissivity of multiyear ice

which depends on the history of the material (and especially on the fraction of contaminants or scatterers in the material) could vary significantly from region to region (Maztler et al., 1984; Grenfell, 1992). Moreover, the signature of second year ice has been observed to be intermediate to those of first year and multiyear ice (Tooma et al., 1975). Time series analysis of satellite data actually suggests that the signature of second year ice is closer to that of first year ice (Comiso, 2006) and overlaps with that of relatively low concentration multiyear ice.

The microwave brightness temperature of sea ice and open water for different frequencies and polarizations varies considerably as illustrated in the 3-D scatter plots in Fig. 2a, which makes use of AMSR-E 36 GHz T_B data at horizontal and vertical polarizations and 89 GHz T_B at vertical polarization. Projections of the 3-D data to the 2-D components are also shown in Fig. 2a with the top left being the 2-D plot of 89 GHz (V) vs 36 GHz (V), top right for 89 GHz (V) vs 36 GHz (H), and bottom plot being 36 GHz (H) versus 36 GHz (V). The cluster of data points in the vicinity of O, represents open water while those near A, C and D represent first year ice, second year ice (or first year ice with thick snow cover) and multiyear ice, respectively. A large scatter of data for the different ice types is apparent reflecting the large variability in the emissivity of the different ice types, especially multiyear ice. The variations in emissivity are in part due to the presence of mixtures of different ice types. The emissivity is shown to be more variable at higher frequencies because of the shorter wavelengths which make the emitted radiation more vulnerable to scattering than those with longer wavelengths.

Large temporal and spatial variability in the microwave brightness temperature of multiyear ice is apparent when scatter plots such as those shown in Figure 2 are plotted for each month. To minimize errors associated with this variability, a dynamic tie point for multiyear ice is used and adjustments are made to account for the observed monthly and yearly variations in the multiyear ice emissivity. To estimate multiyear ice concentration, we assume that the average emissivity of

multiyear and first year ice can be inferred from the data and that the data points in between the averages represent mixtures of multiyear and first year (or second year) ice. The multiyear year concentration is then derived using the following mixing algorithm:

$$T_B(\nu, P) = T_{BFY}(\nu, P)*C_{FY} + T_{BMY}(\nu, P)*C_{MY} + T_{BOW}(\nu, P)*C_{OW} \quad (1)$$

where $T_B(\nu, P)$ is the brightness temperature observed by the satellite at frequency ν and polarization P while $T_{BFY}(\nu,P)$, $T_{BMY}(\nu, P)$ and $T_{BOW}(\nu, P)$ are the inferred brightness temperature at the same frequency and polarization for 100% first year ice, multiyear ice and open water. Also, for each data element, only three types of surfaces are assumed and therefore,

$$C_{FY} + C_{MY} + C_{OW} = 1 \quad (2)$$

Using two AMSR-E channels (i.e., 36 GHz at horizontal and vertical polarizations) in equation (1) we have two equations and together with equation (2), we have the required three equations to estimate three unknowns including the the concentration of multiyear ice. The typical brightness temperature is adjusted every month of the year to account for changes in the emissivity of the surface and the temperature of the ice. An example of a retrieved multiyear ice concentration is shown in Figure 2b. We use a threshold of 30% for multiyear ice concentration to exclude most of the second year ice types as discussed in Comiso (2006) and to get a consistently derived concentration of multiyear ice. Our ability to separate the thicker multiyear ice types from other ice types is surprisingly good as described below.

The scatter plot in Fig. 2a is color coded such that the data elements with multiyear ice cover that is 30% and above is shown in red. The geographical location of the color-coded data is

provided in Fig. 2c with the data elements from the multiyear ice covered region being shown in red while those in the seasonal regions are shown in blue. In the 3-D scatter plot in Fig. 2a, the seasonal ice cover and open water data (black data points) are confined to a plane defined by OAC. On the other hand, the multiyear ice data points are out of this plane and are clearly separate from the other data points. It is thus apparent that the multiyear ice data points have signatures that are unambiguously distinct from the other data points. This is an unexpected but a most welcomed observation because it indicates that retrieved multiyear ice data belongs to a special type that can be separated from the other ice types.

The Bootstrap Algorithm, which has been used only to estimate sea ice concentration (Comiso, 2010), makes use of the cluster of data points that follow a linear pattern along the line AD (see the 36H vs 36V plot at the bottom of Figure 2) to represent near 100% sea ice concentration. The same cluster of data points provides the means to estimate the multiyear ice concentration in winter when the Arctic basin is covered mainly by consolidated ice. We assume that the data in the AD cluster represents mixtures of seasonal and multiyear ice cover with those near the label A representing 100% first year ice while those near the label D representing near 100% multiyear ice. Using the aforementioned mixing algorithm, the concentration of multiyear ice is estimated but instead of the reference points being fixed for all months and all years, as in Gloersen et al. (1992) and Johannessen et al. (1999), we used a dynamic reference point for 100% multiyear ice as indicated earlier. Such adjustment is made based on the frequency distribution of the AD cluster and is done consistently for the entire satellite data set. Monthly averages were used instead of daily data to minimize short-term effects that may be associated with the occurrences of storms and other phenomenon. The adjustments in tie points from November to April enabled retrieval of consistent multiyear ice cover for each month during the winter period.

Monthly multiyear-ice concentration maps derived using aforementioned procedure and January data from 2005 to 2010 are presented in Fig. 3. The images are very similar to those derived from QuikScat data (Ngheim et al., 2007; Kwok et al., 2009). This is not surprising because both passive and active microwave data show a strong contrast in the signature of multiyear ice and first year ice. However, there are subtle differences both at the edges and the interior that may be associated with differences in the sensitivities of the two sensors to different surface types, such as ridged ice, new ice with salt flowers, first year ice and open water. Multiyear ice concentrations from passive microwave data have been derived and studied previously (e.g., Gloersen et al., 1992; Walsh and Zwally, 1990; Johannessen et al, 1999) and although the spatial features of the retrieved values are similar to our retrievals, the magnitudes of the values are different because of differences in the tie-points and technique. The set of images shown in Fig. 3 illustrates how the multiyear ice cover changes from one year to another. The month with the lowest multiyear ice extent is January 2008, which is expected because of the record low perennial ice cover in September 2007. The multiyear ice cover in January 2009 (Fig. 2e) shows a more extensive coverage (by about 10%) than that of January 2008 but it is not as extensive as that of January 2007 (Fig. 2a). A similar image for January 2010 (Fig. 2d) is even more extensive (about 20% higher than January 2008) in part because of enhanced perennial ice cover in September 2009 compared to September 2008. The increases in multiyear extent in 2009 and in 2010 indicate that more second year ice survived the summer melt period than in 2008.

To illustrate the consistency and coherence of the derived data during the winter period and to confirm that the 2010 multiyear ice extent is reflected in other winter months, monthly multiyear ice concentration maps from November 2009 to April 2010 are presented in Figure 4. The images in November and December are very similar but with some discrepancies near the

edges that are likely associated with ice dynamics. From January to March, the unique ice formation (that looks like tongue) near Alaska grew gradually in size. Data from this tongue in March was further analyzed (as was done in Fig. 2) and the results show that the data indeed have multiyear ice signatures. The monthly wind data that is also shown in Fig. 4, suggest that the increase in size of the feature was likely caused by the advection of multiyear ice cover into the region. This is in part supported by preliminary analysis of ice drift data and by results of quantitative analysis (i.e., see next section) that show that the extent and area of the multiyear ice cover did not change much from November 2009 to April 2010.

4. Interannual Variability of Multiyear Ice and Perennial Ice

a. Extent and Area of Multiyear and Perennial Ice

Monthly multiyear ice concentrations were derived during the cold and dry months (November to April) from 1978 to 2010. The monthly ice extent and area of multiyear ice during the period are presented in Figure 5. The plots are color coded (as indicated) to show the value for each month during each ice season. Generally, the values show a decline during the winter season, reflecting the expected loss of multiyear ice that may be caused by the advection of the ice through the Fram Strait to the Greenland Sea and the Atlantic Ocean where they melt. Some increases from November to December can be noted for some years and this is likely in part due to surfaces that were previously wet and did not attain their multiyear ice signature until December. It is encouraging to note, however, that the monthly changes are small compared to the interannual variations.

. It is apparent that during the 1978 to 2010 period, the extent and area of multiyear ice were generally declining. It is however intriguing that during the period, there appears to be an 8 to 9 year periodic cycle (see dash line) as is evident from 1982 to 1991, from 1991 to 2000 and from 2000 to 2008. There are some deviations from this cycle during some years, as in 1987 and 1996, but a cycle of growth and then decline is apparent over each nine-year period. It is thus possible that the observed increase from 2008 to 2009 and then to 2010 is part of this periodic pattern. Further studies are needed but the 8 to 9-year cycle is also similar to the period of the Antarctic Circumpolar Wave (White and Peterson, 1996).

The temporal evolution of the perennial and multiyear ice cover in the Arctic during the last three decades is summarized in the color-coded images presented in Figure 6. The averages for the perennial ice for the periods 1979 to 1988, 1989 to 1998 and 1999 to 2008 are presented in Figs. 6a to 6c while the corresponding averages for multiyear ice (i.e., February 1980 to 1989, February 1990 to 1999 and February 2000 to 2009) are presented in Figs 6e to 6f. The dates are slightly shifted since the perennial ice is observed in September of one year while the corresponding multiyear ice is observed in the subsequent winter. The month of February was chosen to illustrate the decadal variability but results would have been basically the same if December or January averages were used. It is apparent that the averages for the perennial ice cover are considerably more extensive than the corresponding averages in the multiyear ice cover. This is in part because of the 30% threshold used in the multiyear ice algorithm that excludes data elements with low multiyear ice concentrations and a large fraction of the second year ice cover. The perennial ice concentration maps also include a small fraction of new and first year ice that may have formed in some areas during the end of the summer period.

The first set of images shows that the inter-decadal declines in the perennial ice cover occurred mainly near the marginal ice zone. The changes for the perennial ice cover appear to be

a systematic retreat that is especially large in the Beaufort, Siberian, Laptev and Barents Seas. The averages for the third decade show significantly larger areas of ice free water, especially at the Beaufort Sea and the Siberian/Laptev Seas regions, indicating a much larger ice decline from the second to the third decades compared to that of the first two. The trends in the perennial ice cover, as presented in Fig. 6d, show the locations that have been most vulnerable to change. The color-coded map represents results from linear regressions using monthly ice concentration anomalies in each data element (pixel) from 1979 to 2009. It is apparent that the declines are largest in the western regions that include the Beaufort Sea, Chukchi Sea and Siberian Sea. The trends are more moderate in the Eastern region.

The decadal changes in the multiyear ice cover, as depicted in Fig. 6, are considerably greater than those of the perennial ice not just in extent but in shape as well. The averages for the first and third decade show a sharp corner protruding in the Siberian Sea, while the averages for the second decade looks more circular with no distinct patterns at the edges. Such decadal changes in pattern may be associated with inter-decadal changes in the circulation pattern of the sea ice as reported by Proshutinsky and Johnson (1997). The decadal changes in the multiyear ice cover are also shown to be much larger from the second to the third decade than from the first to the second, especially in the Beaufort and Kara/Barents Seas. The trends in the multiyear ice cover as shown in Fig. 6h show that changes were not confined to the marginal ice regions but occurred all the way to the interior regions. The appearance of an approximately linear pattern of negative trend (in red) from the Siberian Sea to Fram Strait in the trend map is conspicuous, especially since linear feature overlaps with the transpolar drift region. This suggests that the ice cover that is advected from the Arctic through Fram Strait has less concentration of multiyear ice in recent years that in earlier years. Such phenomenon needs to be taken into consideration when quantitative estimates of the multiyear ice area exported from the Arctic are being made.

b. Trends in Multiyear and Perennial Ice Cover

The yearly extent and area of the perennial and multiyear ice cover in the Central Arctic (i.e., excluding Greenland Sea multiyear ice cover) are presented in Figure 7. The perennial ice extent and area are derived from data during the summer minimum which occurs usually in September while the corresponding values for multiyear ice cover are averages of the monthly values in the winter period (i.e., December, January and February). The plots show large but similar interannual variability for both perennial and multiyear ice cover. Note that the extent of the perennial ice cover which was as high as about 8 x 10^6 km^2 in the early 1980s went down in value to as low as about 4 x 10^6 km^2 in the latter part of 2000s. Similarly, the multiyear ice extent went down from about 6.2 x 10^6 km^2 in the 1980s to about 2.8 x 10^6 km^2 in the late 2000s. Using linear regression analysis, the trends of the perennial ice extent and ice area were estimated to be strongly negative at -12.2±1.6 %/decade and -13.5±1.6, respectively, for the period from 1979 to 2010. These values are considerably higher than the values reported by Comiso (2002) for an earlier time period. The trends in the multiyear ice extent and area turned out to be even more negative rate at -15.1±1.9 %/decade and -17.2±2.4 %/decade, respectively, for the period from 1981 to 2011. Since data for the full month of February 2011 was not available at this time, we used the average of December 2010 and January 2011 data for the last winter data point. The larger trend in ice area compared to that of ice extent indicates that the concentration of multiyear ice in the perennial ice region has been declining. The rate of decline in the multiyear ice cover is unusually high but is consistent with analysis of ice drift data by Maslanik et al. (2007) suggesting that the thickest and oldest ice type in the Arctic has been declining significantly.

The higher negative trend for the thicker multiyear ice area than that for the perennial ice area also implies that the average thickness of the ice cover, and hence the ice volume, has also been declining. These results are consistent with the reported decline of ice thickness as observed from submarine data (Rothrock et al., 1999; Wadhams and Davis, 2000) and satellite data (Kwok and Rothrock, 2009).

5. Connections with Surface Temperature, Sea Level Pressure and Winds

a. Surface Temperature

Decadal averages of Arctic surface temperature as derived from AVHRR data using the technique discussed in Comiso (2010) are presented in Fig. 8a, 8b and 8c for the first, second and third decades, respectively. The decadal averages, show that at least for the last three decades, the spatial distribution and patterns of the isotherms and the location of extremely cold and warm areas are basically the same. Significant decadal changes, however, occurred as revealed by the differences of the first and second decades (Fig. 8d) as well as those for the second and third decades (Fig. 8e). It is also shown that although the differences are dominantly positive (i.e., indicating warming) especially in North America, there are regions where some cooling has been concurrently going on. For example, in Fig. 8d, cooling is apparent mainly in the western part of Russia and the Barents Sea region. Some cooling also occurred in parts of Greenland, North America and the Bering Sea. In Fig. 8e, cooling was more widespread in Russia, becoming more expansive to the western region, including the Sea of Okhotsk and the Bering Sea. The anomalies in the Central Arctic region, North America and Greenland, however, became more dominantly positive with extreme values occurring in the Baffin Bay and Barents Sea, reflecting

sea ice retreats in these regions during the period. The difference map between the first and the third decades (Fig. 8f) show higher positive values than those shown in Figs 8d and 8e, indicating that the third decade was considerably warmer than the first decade and significantly warmer than the second decade. The difference map indicates that some cooling is apparent in parts of eastern Russia and the Bering Sea. On the other hand, the extremely high positive values have expanded to include Greenland Sea and Hudson Bay, which are areas where the sea ice cover has declined significantly during the last three decades.

A more quantitative evaluation of the interannual variability of surface temperature is presented in the plots of temperature anomalies and for different regions of the Arctic at >60^{o}N (Fig. 9). The anomalies show large interannual fluctuations and even some periodic but not consistent patterns in some regions. The trends from linear regression analyses are consistently positive but vary significantly in value from one region to another with the trends being 0.68 ± 0.07, 0.69 ± 0.12, 0.12 ± 0.09 and 0.59 ± 0.10 ^{o}C/decade, for sea ice, Greenland, Eurasia, and North America, respectively. The yearly averages are also shown in Fig. 9 and there is a suggestion of a periodic cycle in North America.

For direct comparison of sea ice with surface temperature, monthly anomalies of sea ice area and surface temperature over sea ice in some sectors of the Arctic (as described in Parkinson et al., 1999) are presented in Figure 10. The sectors are those in the Central Arctic and adjacent seas (i.e., Kara/Barents Seas, Okhotsk/Japan Seas, Bering Sea and Greenland Sea). The trend in the sea ice cover is generally negative in regions where the trends in surface temperatures is positive for all sectors except in the Bering Sea sector which is the only sector where the trend in the sea ice cover is positive at 4.5±1.6 %/decade. In this case, although there are areas where cooling has been observed (i.e., Fig. 8), the net trend in surface temperature is slightly positive at 0.15±0.05 ^{o}C/decade. In the Kara/Barents Seas, Okhotsk Sea and the Greenland Seas, the trends

in the sea ice extent are -9.8±0.7, -9.6±0.17, and -8.0±0.8%/decade, respectively, while the corresponding trends in surface temperatures are 0.94±0.09, 0.41±0.05 and 0.77±0.03 ^{o}C/decade. In these regions, the trends in surface temperature are highly consistent with the trends in the sea ice cover. In the Central Arctic, the trend in ice extent is -2.0±0.2 %/decade while that of surface temperature is 1.1±0.10 ^{o}C/decade. In this case, despite the relatively high trend in surface temperature, the negative trend is ice area is relatively weak because the ice anomalies in the region are near zero most of the year because of near 100% ice cover.

Scatter plots of sea ice area versus surface temperature for each of the five sectors (not shown) show negative linear patterns indicating strong correlation between the two variables. The results of regression analysis shows that data in the Bering Sea Sector actually have the highest correlation with correlation coefficient of -0.796 while those of the Kara/Barents Seas, Greenland Sea and Okhotsk Sea following closely with -0.784, -0.754, and -732, respectively. The high correlation between the two variables is a manifestation of the strong influence of surface temperature on the sea ice cover. In the Central Arctic region, the correlation coefficient is significant at -0.641 but relatively lower than the other three in part because for most of the year, the sea ice area is almost constant and near maximum values while the surface temperature fluctuates significantly. The surface temperature data, however, shows warming anomalies, not just in the seasonal ice regions but also in the perennial ice region and adjacent land and sea areas. The general warming in these areas would increase the length of the melt season as reported by Markus et al. (2009) and shorten the length of the ice season that in turn causes the ice cover to be generally thinner than normal.

For completeness, changes in SST were evaluated using the AVHRR data from 1981 to 2010 at high latitude regions (i.e., >60^{o}N) of the Arctic and for the Eastern (Atlantic side) and Western (Pacific Side) regions. Except for a few exceptions, the yearly fluctuations are usually less than a

^{o}C. The trend for the entire Arctic region was estimated to be 0.24±0.02^{o}C/decade while those for the Eastern and Western Regions were 0.22±0.03 and 0.25±0.02 ^{o}C per decade, respectively. The relatively high trends in SST suggest a significant influence of ice-albedo feedback associated with the rapid decline in the summer ice cover during the last three decades. This is consistent with previous studies (Perovich et al., 2008; Lindsay et al., 2009). The AVHRR data also show that the SST in the Western Arctic was abnormally high in 2007 and consistent with observations using passive microwave data by Shibata et al. (2010).

b. Sea Level Pressure and Winds

To assess how changes in atmospheric wind patterns and SLP alter the distribution and influence the interannual changes in the sea ice cover we make use of the NCEP reanalysis data set as discussed by Kalnay et al (1996). Decadal averages of sea level pressure (SLP) and winds for a winter month (February) are presented in Fig. 11. The spatial patterns of the SLP distributions for the three decades are shown to be similar with the highs generally in the Central Arctic Region, Russia, North America and Greenland and the lows in the North Atlantic and North Pacific regions. From the first to the second decade, the lows in the North Atlantic expanded and moved to the East. From the second to the third decades, the North Atlantic lows retreated to the west though not as far back as in the first decade. Meanwhile, the lows in the North Pacific deepened from the first to the second decade and also from the second to the third decade. The results of trend analysis of the pressure fields are presented in Figure 11d and show that the highs were further enhanced in the Central Arctic while the lows deepened in both North Pacific and North Atlantic. The wind patterns show subtle changes from one decade to another but overall, the trend in the Central Arctic is a net increase in northerly winds. This would cause

sea ice near the poles to be advected to the south, primarily to the southern Beaufort, Siberian and Laptev Seas where they are likely to melt in the summer.

Periodic changes from the typical anti-cyclonic to cyclonic wind circulation has been suggested in various studies (i.e., Proshutinsky and Johnson, 1997; Asplin et al., 2009) but during the satellite era, starting in 1978, such periodicity has not been consistently observed. The data shown in Figure 11 show some but not dramatic changes in wind direction from one decade to another. The decadal averaging, however, may not provide information about the actual changes that may occur at shorter time periods. The atmospheric circulation patterns are important to monitor since some wind patterns are favorable to the advection of multiyear or thick ice through Fram Strait and eventually to the Atlantic Ocean where they melt. Such events could cause significant interannual changes in the extent of the multiyear ice cover.

It has been postulated by Johnson and Wallace (1996) that the atmospheric circulation pattern in the Arctic is controlled by the Arctic Oscillation (AO). The AO has been quantified through the use of the AO indices which are the differences of the SLP of an annular region in the upper mid-latitude region (>40^{o}N) in the Northern Hemisphere and the Central Arctic region. Using data provide by the NOAA Cliamte Prediction Center, monthly AO indices from November 1978 to December 2010 are presented in Fig. 12a, while yearly averages of AO indices for each winter (DJFM) from 1979 to 2010 are presented in Fig. 12b. Negative AO indices (e.g., 1979 to 1988) have been associated with relatively high extents in the sea ice cover while positive indices (e.g., 1989 to 1995) have been associated with relatively low extents in the ice cover (Rigor et al., 2002). However, since 1996, the indices have not been consistent and would go from negative to positive and back to negative from one year to another. The AO was regarded as basically neutral during the last decade (Overland and Wang, 2005) and led others to postulate a radical shift in the atmospheric circulation (Zhang et al., 2008). During this time period, the sea ice

cover continued to decline after a peak value in September 1996 (see Fig. 1a). The high variability of the ice extent in 2007, 2008, 2009 and 2010 and the anomalously low values in September during each of these years are also shown to be unprecedented. The AO indices were positive (but not as high as in 1989 and 1990) during this period until they dropped down to record low values in 2010. The impact of such a drop in AO index on the sea ice cover would be interesting to know but is not clearly manifested in the current ice data.

The results of correlation analysis of the data show a relatively weak relationship between the sea ice cover and AO indices. Using monthly data in winter, autumn and spring (October to April) from 1978 to 2010, regression analysis yielded a correlation coefficient for AO versus sea ice extent and AO versus sea ice area, of 0.021 and 0.014, respectively. The relationship is even weaker when the yearly winter AO indices were regressed versus multiyear extents and multiyear ice areas since they yielded -0.0026 and 0.0006, respectively. Both results indicate that a direct correlation between the two variables does not exist. However, this does not mean that the AO does not affect the sea ice cover. The general location and distribution of the perennial ice and the multiyear ice cover depends on the atmospheric circulation which is controlled by the AO. During some years, the perennial ice cover is advected to the west causing a limited area of open water in the region while during other years the ice is advected to the east causing a large area of open water to occur in the Beaufort Sea region in the summer. The location and environment can make a difference in terms of the rate of melt of sea ice.

6. Discussion and Conclusions

Satellite observations of the perennial ice cover in the Arctic region have provided some of the most convincing evidence of a rapidly changing Arctic. The updated values for the trends in the extent and area of the perennial ice are -12.2% and -13.5 %/decade, respectively, revealing

stronger negative trends than previously reported. The analysis of the thick component of the perennial ice, called multiyear ice, as detected by satellite data in winter, yielded an even more rapid rate of -15.1 and -17.2 % per decade for the multiyear ice extent and ice area, respectively. The much higher rate of decline of the multiyear ice than the perennial ice cover is clearly an indication that the average thickness of the Arctic ice cover is declining. Such decline in the thick component of the Arctic ice cover means an even more vulnerable perennial ice cover. It is interesting that the rates of decline are so strongly negative despite slight recoveries in the last three years from the anomalously low values in 2007 and 2008 for perennial and multiyear ice, respectively.

We note that the dramatic decline of the perennial ice cover from 2006 to 2007 is not reflected in the multiyear ice data. The multiyear ice data show a monotonic and gradual decline from 2003 to 2008 suggesting that the anomalously low perennial ice cover in 2007 was likely due in part to the melt of a large fraction of the second year ice in the same summer. This also mean that the interannual variability in the perennial ice cover is partly controlled by the interannual variability of the second year ice cover. It is intriguing that the multiyear ice data show an indication of a periodic cycle of about 8 to 9 years which is similar to the period of the Antarctic circumpolar wave. Such cycle could explain the slight recovery over the last three years.

Results of regression analyses also indicate that changes in the sea ice cover are strongly correlated with the changes in the surface temperature. The correlation coefficients are however not that high, averaging around 0.75 for the different sectors in the seasonal regions. This indicates that the sea ice cover is controlled by factors other than temperature. The correlation is not as high in the Central Arctic because the ice concentration in the Central Arctic does not change much and is basically close to 100% except in the summer period, even in periods when the surface temperature is highly fluctuating. Sea surface temperatures in ice free areas in the

Arctic basin were also unusually high in 2007 when the dramatic decline in the perennial ice cover occurred. This suggests an important role of ice-albedo feedback in the event. The results of comparative analysis of sea ice and multiyear ice area with AO indicate a much weaker correlation. However, the direct role of AO on the sea ice cover is difficult to quantify by direct correlation analysis. AO influences the pressure and wind patterns that in turn determines the location of the multiyear ice cover in the winter and summer. Multiyear ice located in generally warm ocean areas are likely more vulnerable to melt that those located in colder regions.

Acknowledgements. The author is thankful to R. Gersten of RSI/SESDA-2 and L. Stock of STX for excellent programming and analysis support. This work was funded by NASA's Cryospheric Sciences Program.

References:

Asplin, M. G., J. V. Lukovich, and D. G. Barber, 2009: Atmospheric forcing of the Beaufort Sea ice gyre: Surface pressure climatology and sea ice motion. *J. Geophys. Res.,* **114**, C00A06, doi:10.1029/2008JC005127.

Comiso, J.C., 1990: Arctic multiyear ice classification and summer ice cover using passive microwave satellite data, *J. Geophys. Res.,* **95**, 13411-13422,13593-13597.

Comiso, J. C., 2002: A rapidly declining Arctic perennial ice cover. *Geophys Res. Letts.,* **29***, 1956, doi:10.1029/2002GL015650*.

Comiso, J.C., 2006: Impacts of the variability of 2nd year ice types on the decline of the perennial ice cover, *Ann. of Glaciology, 44,* 375-382.

Comiso, J.C., 2010: *Polar Oceans from Space,* Springer Publishing, New York, doi 10.1007/978-0-387- 68300-3.

Comiso, J.C., C.L. Parkinson, R. Gersten, and L. Stock, 2008: Accelerated decline in the Arctic sea ice cover. *Geophy. Res. Lett.* **35**, L01703, doi:10.1029/2007GL031972.

Eppler, D., M.R. Anderson, D.J. Cavalieri, J.C. Comiso, L.D. Farmer, C. Garrity, P. Gloersen, T. Grenfell, M. Hallikainen, A.W. Lohanick, C. Maetzler, R.A. Melloh, I. Rubinstein, C.T. Swift, C. Garrity, 1992: "Passive microwave signatures of sea ice," Chapter 4, *Microwave Remote Sensing of Sea Ice*, (ed. by Frank Carsey), American Geophysical Union, Washington, D.C., 47-71.

Gloersen P., W. Campbell, D. Cavalieri, J. Comiso, C. Parkinson, H.J. Zwally, 1992: *Arctic and Antararctic Sea Ice, 1978-1987: Satellite Passive Microwave Observations and Analysis.* NASA Spec. Publ. ***511.***

Grenfell, T. C., 1992: Surface based passive microwave studies of multiyear ice. *J. Geophys. Res.* **97**, 3485-3501.

Johannessen, O. M., E. V. Shalina, and M. W. Miles, 1999: Satellite evidence for an arctic sea ice cover in transformation. *Science,* **286**, 1937-1939.

Kay, J.E., T. L'Ecuyer, A. Gettelman, G. Stephens, and C. O'Dell, 2008: The contribution of cloud and radiation anomalies to the 2007 Arctic sea ice extent minimum. *Geophys. Res. Lett.*, **35**, L08503, doi:10.1029/2008GL033451.

Kalnay E, R. Kanamitsu, R. Krisler, W. Collins, D. Deaven, L. Gandin, M. Iredell, S. Saha, G. White, J. Wollen, Y. Zhsu, M. Chella, J. Janowlak, W. Eb, C. R. Ropelewski, R. Jenne, 1996: The NCEP/NCAR reanalysis project. *Bull. Amer. Meteor. Soc*. **77**, 437-479.

Kwok, R., 2008: Summer sea ice motion from the 18 GHz channel of AMSR-E and the exchange of sea ice between the Pacific and Atlantic sectors. *Geophys. Res. Lett.,* **35,** L03504, doi:10.1029/2007GL032692.

Kwok , R. and D.A. Rothrock, 2009: Decline in Arctic sea ice thickness from submarine and

ICESat records: 1958–2008. *Geophys. Res. Lett.*, **36**, L15501, doi:10.1029/2009GL039035.

Lindsay, R.W., J. Zhang, A. Schweiger, M. Steele, and H. Stern, 2009: Arctic sea ice retreat in 2007 follows thinning trend. *J. Climate*, **22**, 165-176.

Markus , T., J. C. Stroeve, and J. Miller, 2009: Recent changes in Arctic sea ice melt onset, freezeup, and melt season length. *J. Geophys. Res.*, **114**, C12024, doi:10.1029/2009JC005436.

Maslanik, J.A., C. Fowler, J. Stroeve, S. Drobot, J. Zwally, D. Yi, and W. Emery, 2007: A younger, thinner Arctic ice cover: Increased potential for extensive sea-ice loss, *Geophys. Res. Lett.*, **34**, L24501, doi:10.1029/2007GL032043.

Matzler, C., R. O. Ramseier, and E. Svendsen, 1984: Polarization effects in sea ice signatures, *IEEE J. Oceanic Engineering*, **OE-9**, 333-338.

Nghiem, S.V., I.G. Rigor, D.K. Perovich, P. Clemente-Colon, J.W. Weatherly, and G. Neumann, 2007: Rapid reduction of Arctic perennial sea ice. *Geophys. Res. Lett.*, **34**, L19504, doi:10.1029/2007GL031138.

Ogi , M., I.G. Rigor, M.G. McPhee, and J.M. Wallace, 2008: Summer retreat of Arctic sea ice: Role of summer winds. *Geophys. Res. Lett.*, **35**, L24701, doi:10.1029/2008GL035672.

Overland, J.E., and M. Wang, 2005: The Arctic climate paradox: The recent decrease of the Arctic Oscillation. *Geophys. Res. Lett*., **32**, L06701, doi:10.1029/2004GL021752.

Perovich, D. K, J. A. Richter-Menge, and K. F. Jones, B. Light, 2008: Sunlight, water and ice: Extreme Arctic sea ice melt during the summer of 2007. *Geophys. Res. Lett.,* **35**, L11501, doi:10.1029/2008GL034007.

Proshutinsky, A. Y., and M. A. Johnson, 1997: Two circulation regimes of the win-driven Arctic Ocean. *J. Geophys. Res.,* **102**, 12,493-12,514.

Proshutinsky, A. Y., R. H. Bourke, and F. A. McLaughin, 2002: The role of the BG in Arctic

climate variability: Seasonal to decadal climate scales. *Geophys. Res. Lett.,* **29**(23), 2100, doi:10.1029/2002/2002GL015847.

Rigor, I.G., J.M. Wallace, and R. Colony, 2002: Response of sea ice to the Arctic Oscillation. *J. Climate*, **15**, 2648-2663.

Rothrock, D. A., Y. Yu, G. Maykut, 1999: Thinning of the Arctic sea-ice cover. *Geophys. Res. Lett.,* **26**, 3469-3472.

Schweiger , A.J., J. Zhang, R.W. Lindsay, and M. Steele, 2008: Did unusually sunny skies help drive the record sea ice minimum of 2007? *Geophys. Res. Lett.*, **35**, L10503, doi:10.1029/2008GL033463.

Serreze, M.C, 2009: The emergence of surface-based Arctic amplification. *The Cryosphere*, 3, 11–19.

Shibata, A., H. Murakami, and J. Comiso, 2010: Anomalous Warming in the Arctic Ocean in the Summer of 2007. *Japan J. Remote Sensing Society of Japan,* **30**(2), 105-113.

Simmonds, I., C. Burke, and K. Keay, 2008: Arctic climate change as manifest in cyclone Behavior. *J. Climate*, **21**, 5777-5796.

Steele, M., W. Ermold, and J. Zhang, 2008: Arctic Ocean surface warming trends over the past 100 years. *Geophys. Res. Lett.*, **35**, L02614, doi:10.1029/2007GL031651.

Stroeve J, M. M. Holland, W. Meier, T. Scambos, M. C. Serreze, 2007: Arctic sea ice decline: Faster than forecast. *Geophys Res Lett.,* **34**, L09501, doi:10.1029/2007GL0029703.

Tooma, S.G., R. A. Mennella, J. P. Hollinger and R. D. Ketchum, Jr., 1975: Comparison of sea-ice type indentification between airborne dual-frequency passive microwave radiometry and standard laser/infrared techniques. *J. Glaciol.,* **15**, 225-239.

Vant, M. R., R. O. Ramseier, V. Makios, 1978: The complex-dielectric constant of sea ice at frequencies in the range 0.1-40 GHz. *J. Appl. Phys*., **49,** 1234-1280.

Walsh, J. E., and H. J. Zwally, 1990: Multiyear sea ice in the Arctic: Model- and satellite-derived. *J. Geophys. Res.*, **95**, 11,613-11,628.

Wadhams P., and N. R. Davis, 2000: Further evidence of ice thinning in the Arctic Ocean. *Geophys Res Lett*., **27**, 3973-3975.

White W. B., R. G. Peterson, 1996: An Antarctic circumpolar wave in surface pressure, wind, temperature and sea ice extent. *Nature*, **380**, 699-702.

Weeks W. F., S. Ackley, 1986: The growth, structure and properties of sea ice. In: Untersteiner (ed) *The Geophysics of Sea Ice*, Plenum, New York.

Zhang, J., R. Lindsay, M. Steele, A. Schweiger, 2008: What drove the dramatic retreat of arctic sea ice during summer 2007? *Geophys. Res. Lett.*, **35**, L11505, doi:10.1029/2008GL034005.

Zhang, X., A. Sorteberg, J. Zhang, R. Gerdes, and J. Comiso, 2008: Atmospheric circulation signature in recent rapid Arctic climate system change. *Geophys. Res. Lett.,* **35**, L22701, doi:10.1029/2008GL035607.

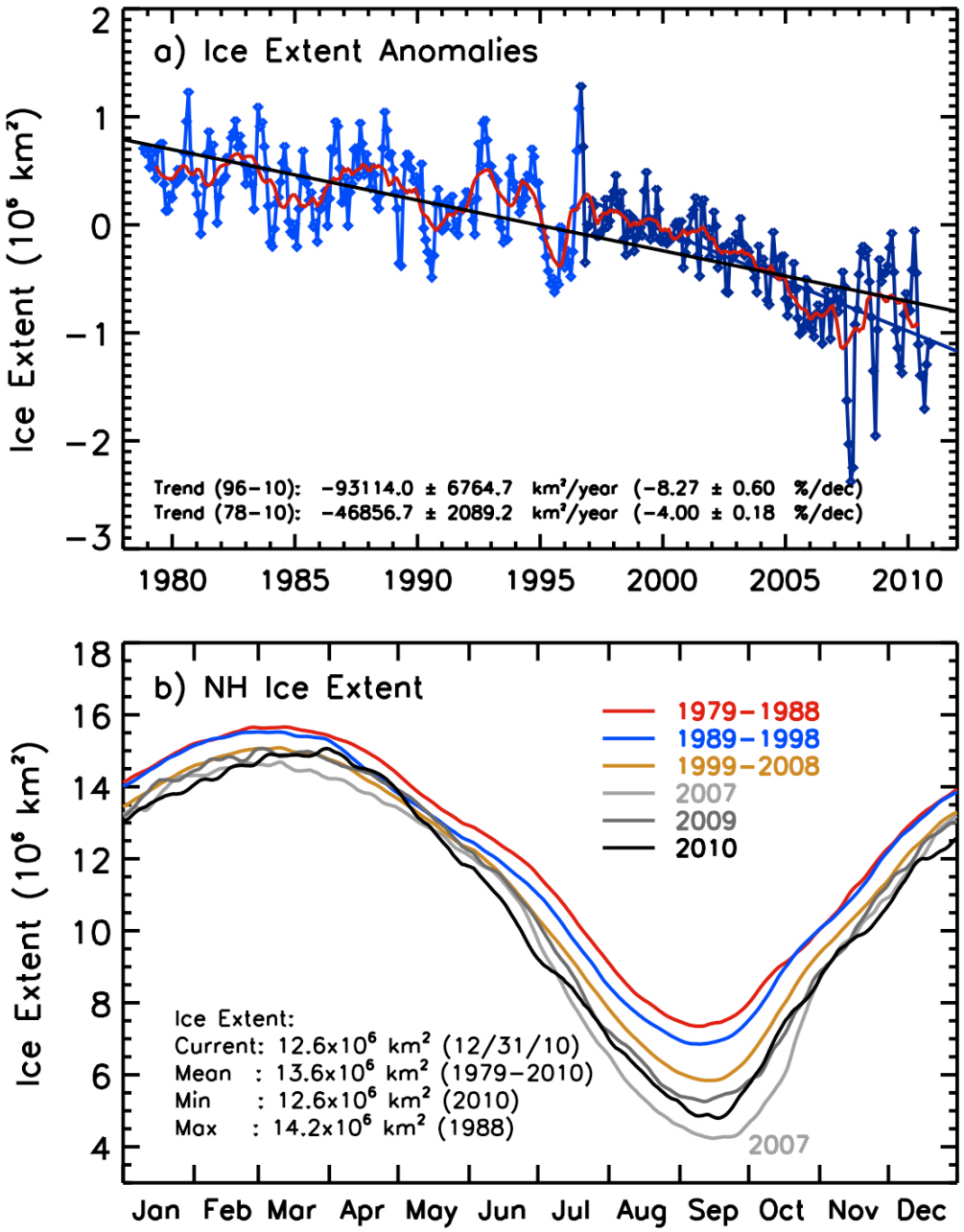

Figure 1. (a) monthly anomalies of the extent of the sea ice cover in the Northern Hemisphere; (b) 10-year averages of daily ice extents and daily ice extents in 2007, 2009, and 2010.

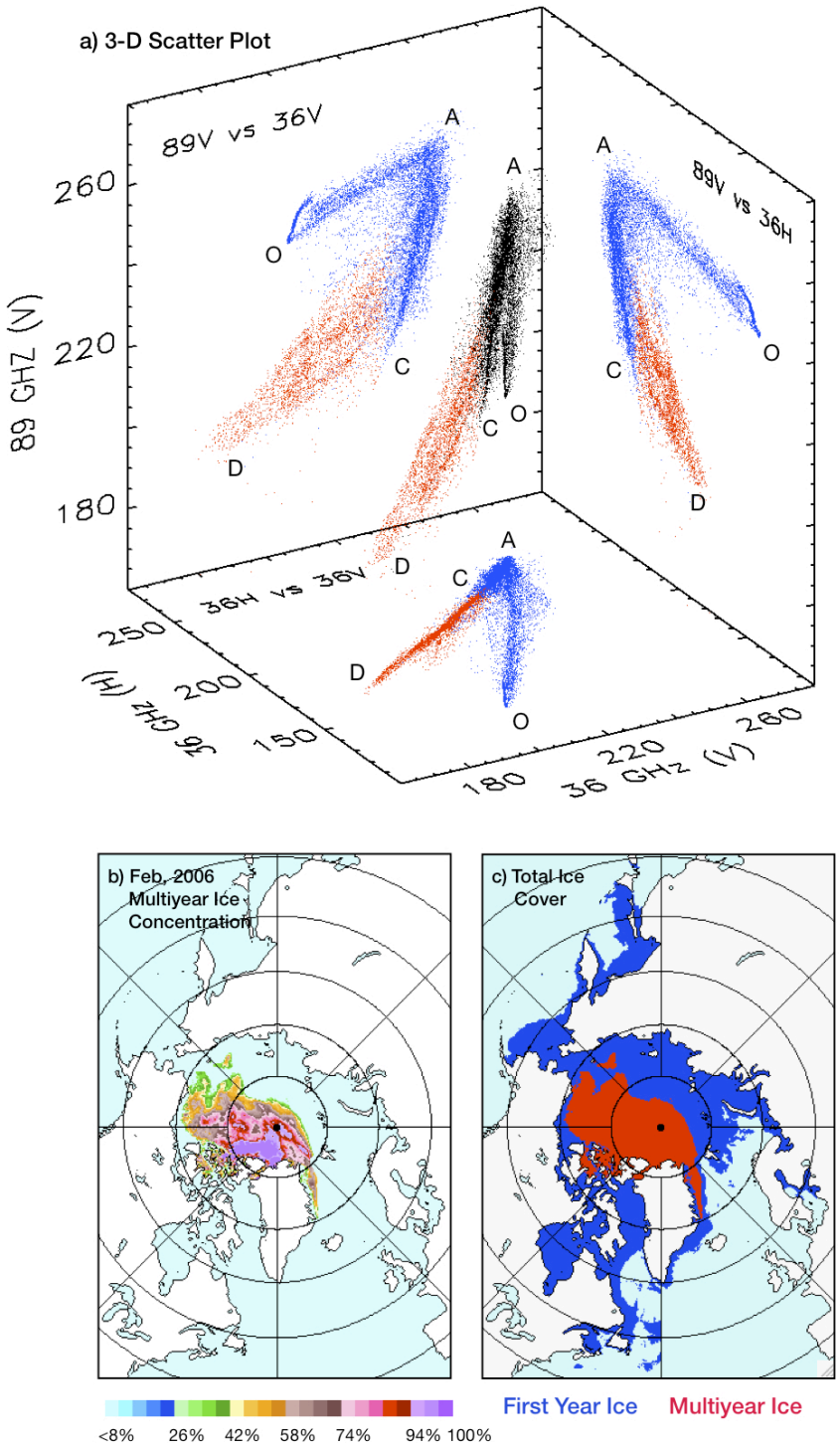

Figure 2. 3-D scatter plot of 37 GHz (V) vs 37 GHz(H) vs 89 GHz(V) using AMSR-E data. 2-D projections of each pair of channels are also shown. (b) derived multiyear ice concentration map for February 2006 and (c) winter ice cover with the location of multiyear ice with ice concentration of 30% or more shown in red while the seasonal ice is shown in blue. In the 3-D scatter plot, the data points representing multiyear ice cover with 30% ice concentration or more are also represented in red.

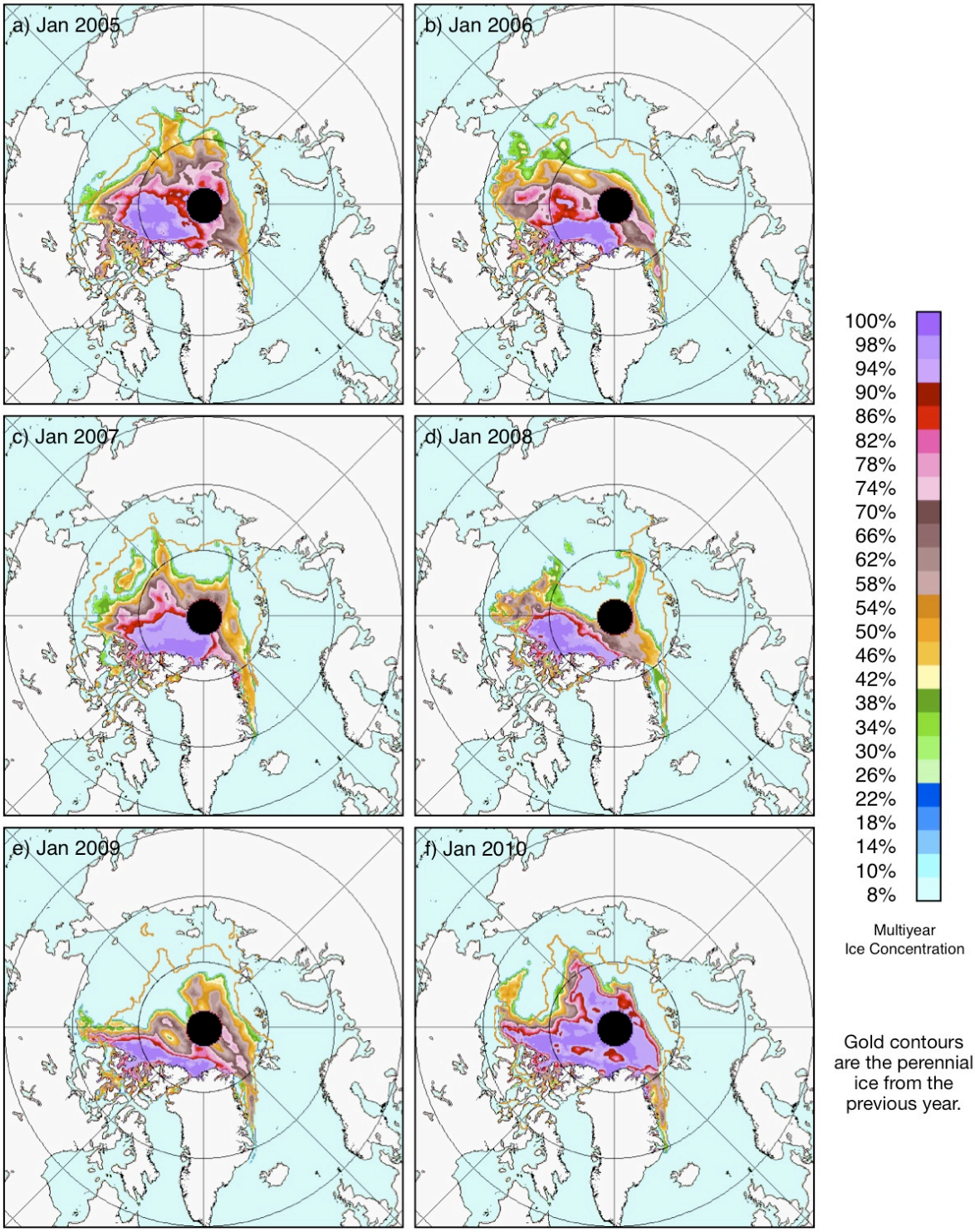

Figure 3. Color-coded multiyear ice concentration maps for each January from 2005 through 2010. The contour lines in gold color represent the 15% ice edge of the perennial ice cover as inferred from the sea ice cover minima the previous summer.

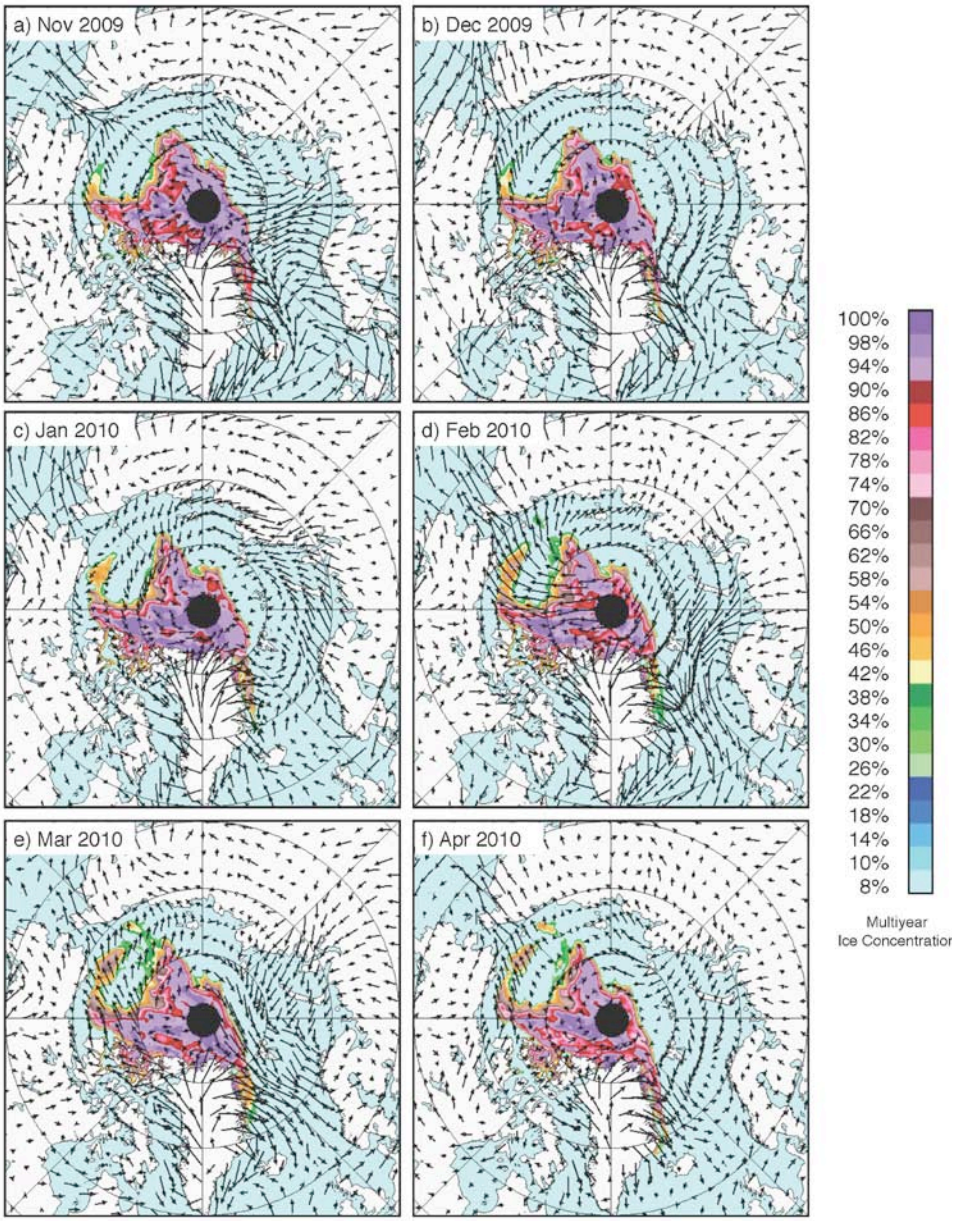

Figure 4. Color-coded multiyear ice concentration maps for each month from November 2009 to April 2010 as inferred from AMSR-E data and the corresponding monthly average wind vectors (from NCEP reanalysis data).

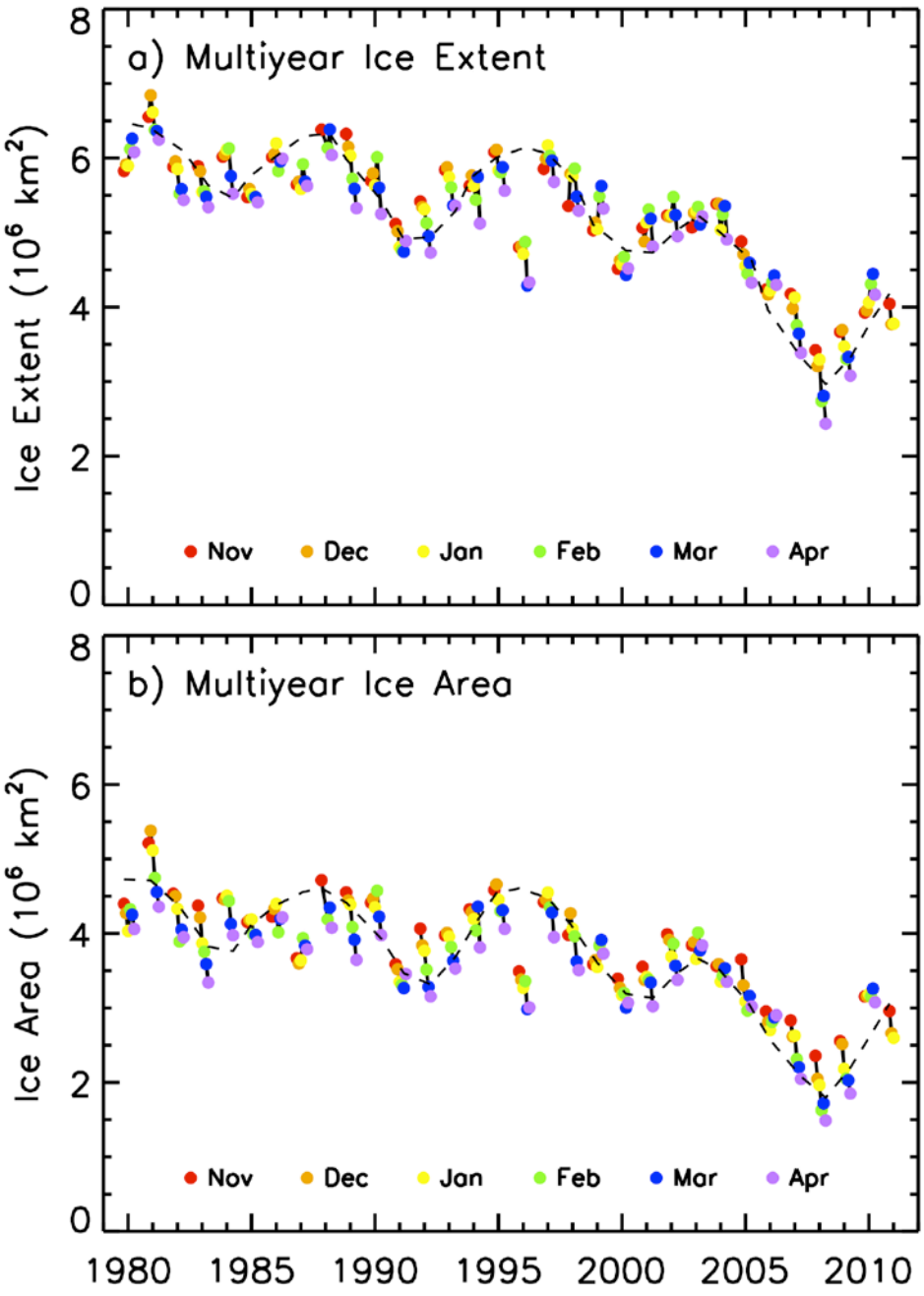

Figure 5. Multiyear ice extent (a) and ice area (b) for the dry months of November to April from 1978 to 2010. The different months are color coded. The dash lines are hand drawn to illustrate that there may be a periodicity in the pattern of about 8 to 9 years.

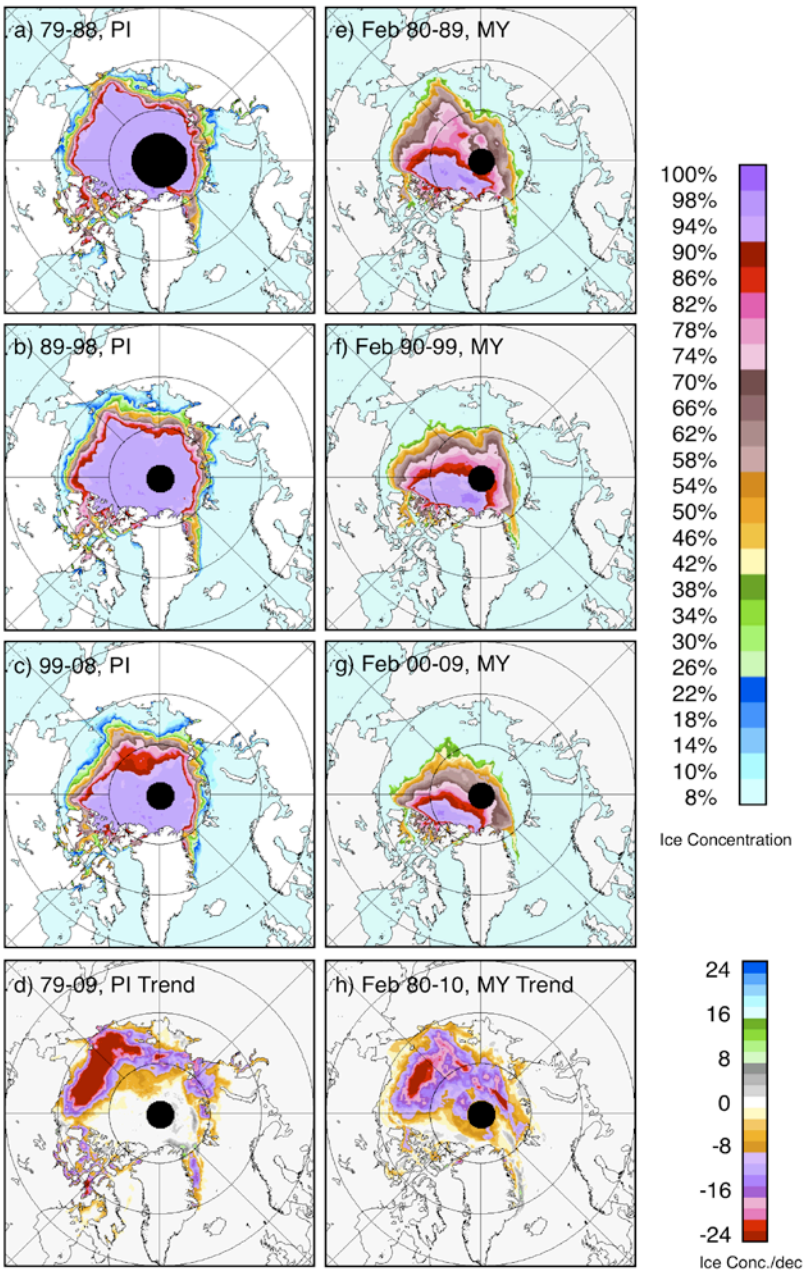

Figure 6. Ten-year averages of the perennial (a to c) and multiyear (e to g) ice cover and trends in (d) the perennial ice from 1979 to 2009 and (h) the multiyear ice from 1980 to 2010. The monthly February data is used to represent multiyear ice for the winter period. The use of other winter months would not change the images significantly.

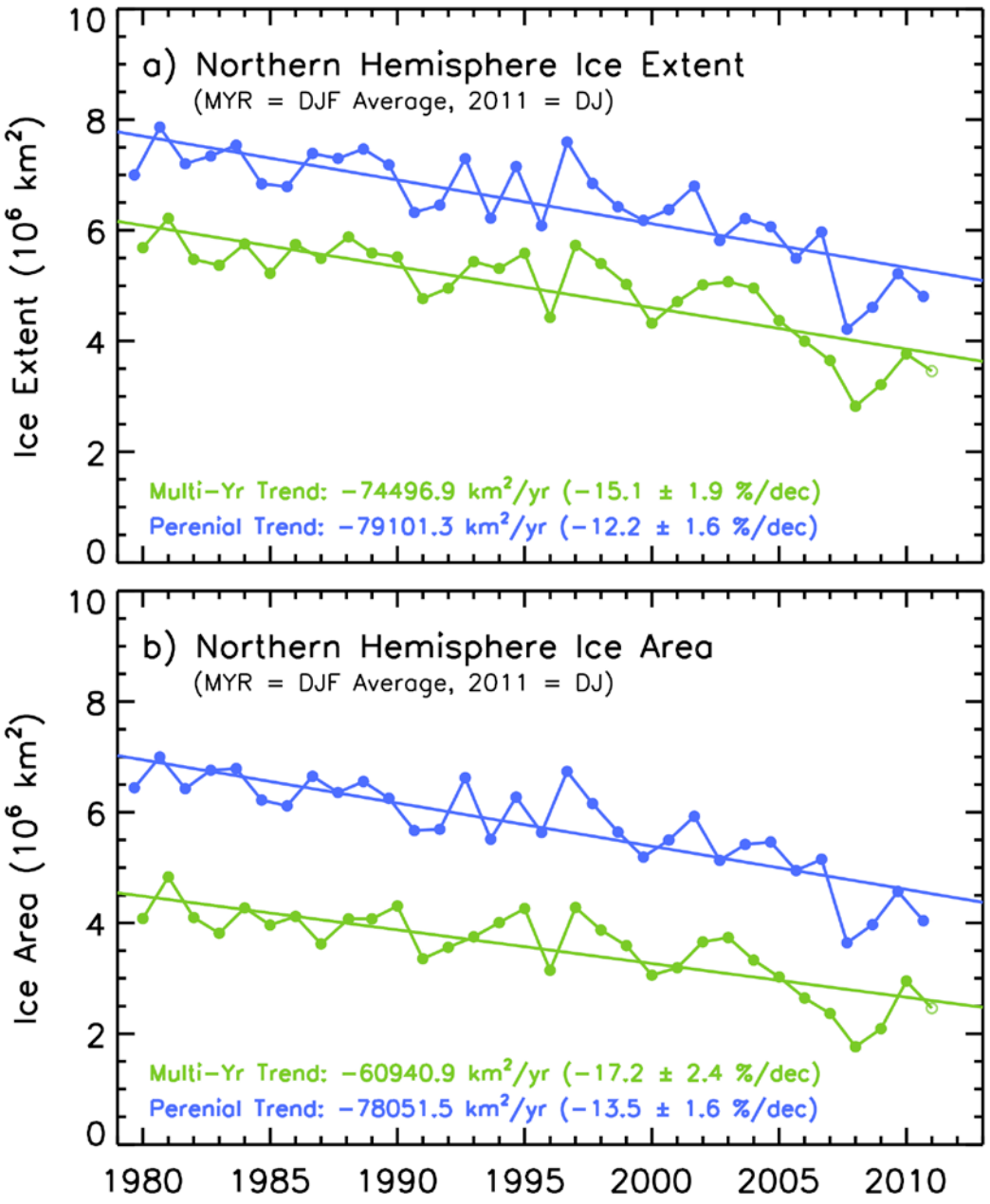

Figure 7. Perennial and multiyear ice extent (a) and ice area (b) for each year from 1979 to 2010. The values plotted for multiyear ice are averages of December, January and February values. The last data point for multiyear ice is for the month of November only. The multiyear ice cover in the Greenland Sea was excluded in the estimates.

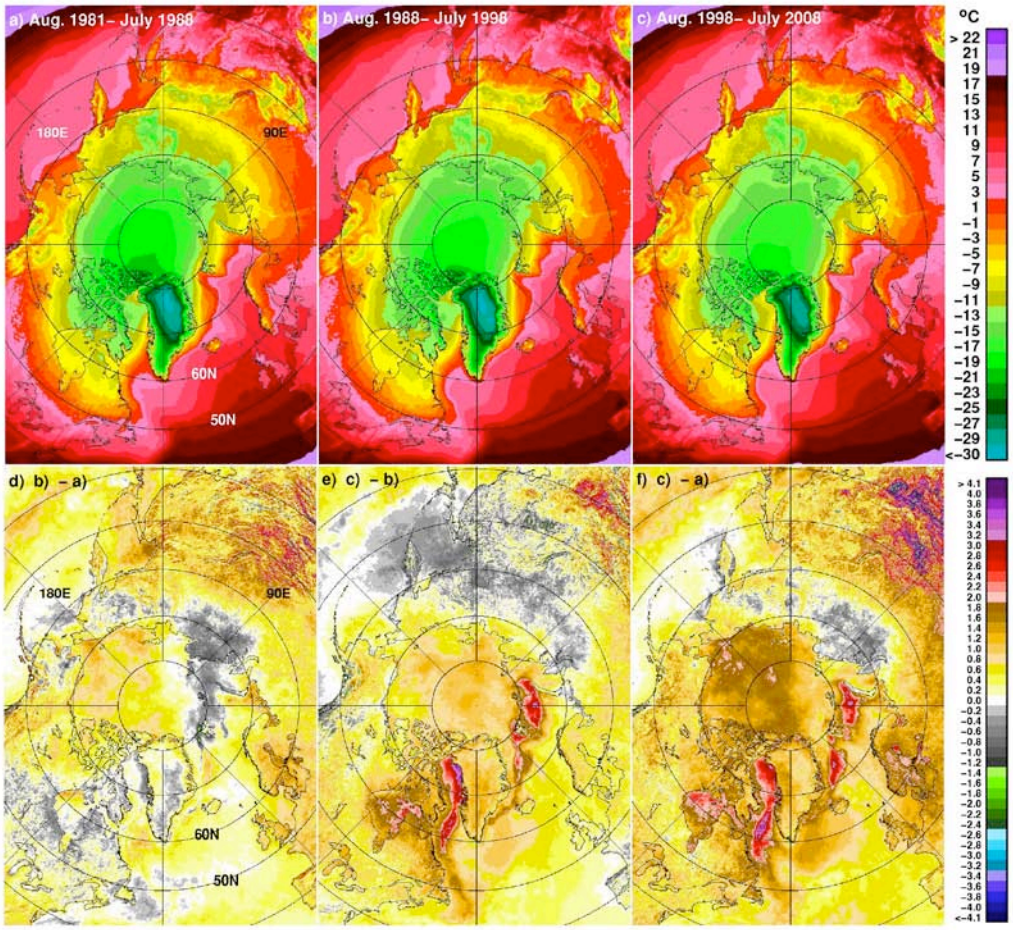

Figure 8. Multiyear averages of surface temperature in the Arctic region for the periods: (a) August 1981 to July 1989; (b) August 1989 to July 1999; and (c) August 1999 to July 2009 and difference maps for (d) map (b) minus map (a); (e) map (c) minus map (b); and (f) map (c) minus map (a).

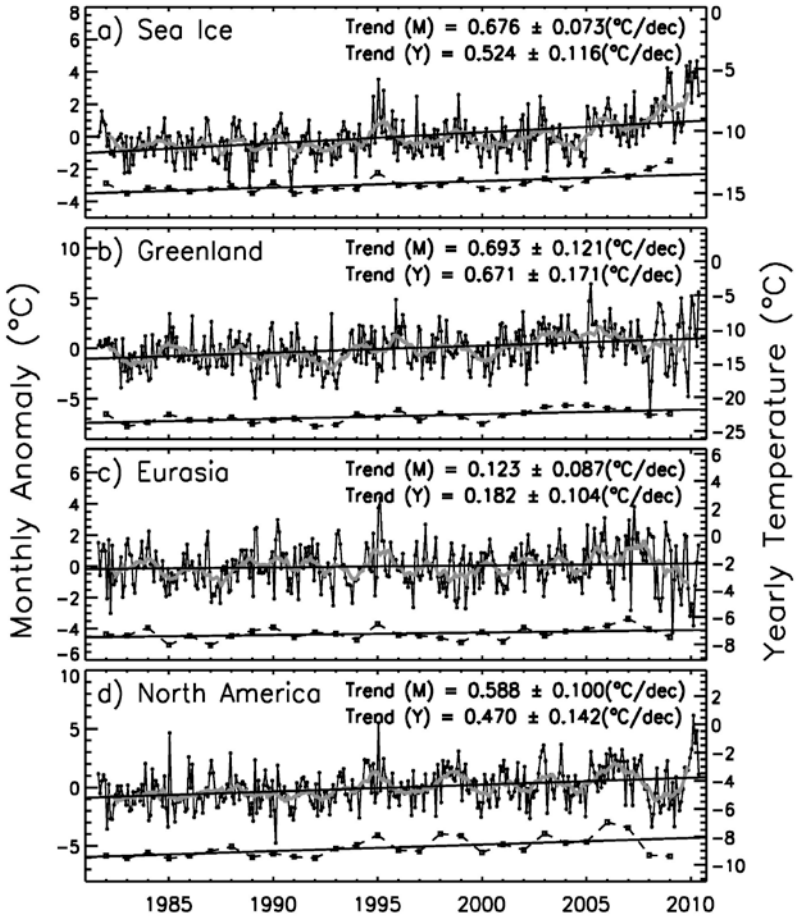

Figure 9. Monthly surface temperature anomalies and yearly averages at >60^{o}N over (a) sea ice; (b) Greenland; (c) Eurasia and (d) North America and estimated trends.

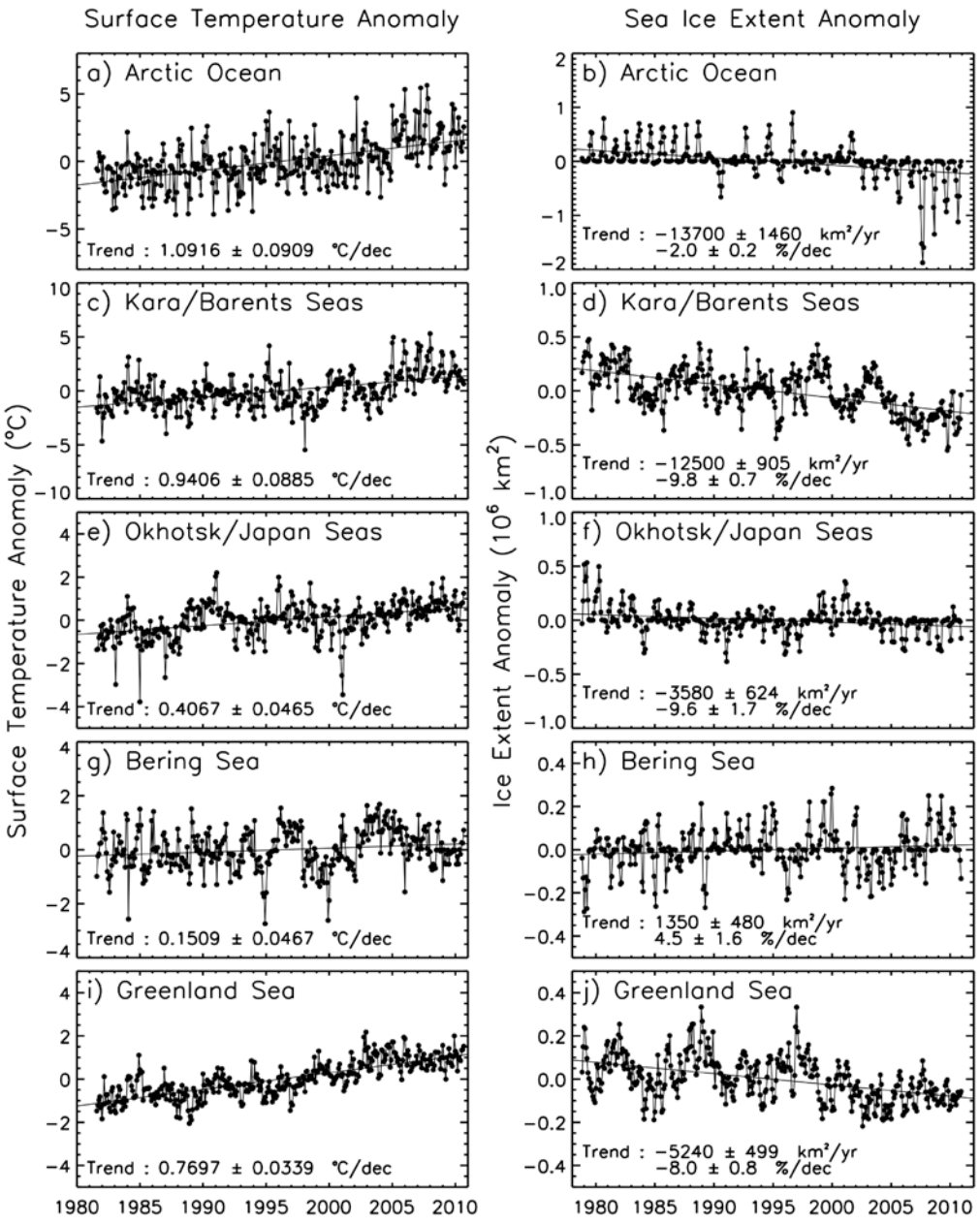

Figure 10 Monthly surface temperature anomalies in (a) Arctic Ocean; (c) Kara/Barents Sea; (e) Okhotsk/Japan Seas; (g) Bering Sea; and (i) Greenland Sea and Ice Area anomalies in (b) Arctic Ocean; (d) Kara/Barents Sea; (f) Okhotsk/Japan Seas; (h) Bering Sea; and (j) Greenland Sea.

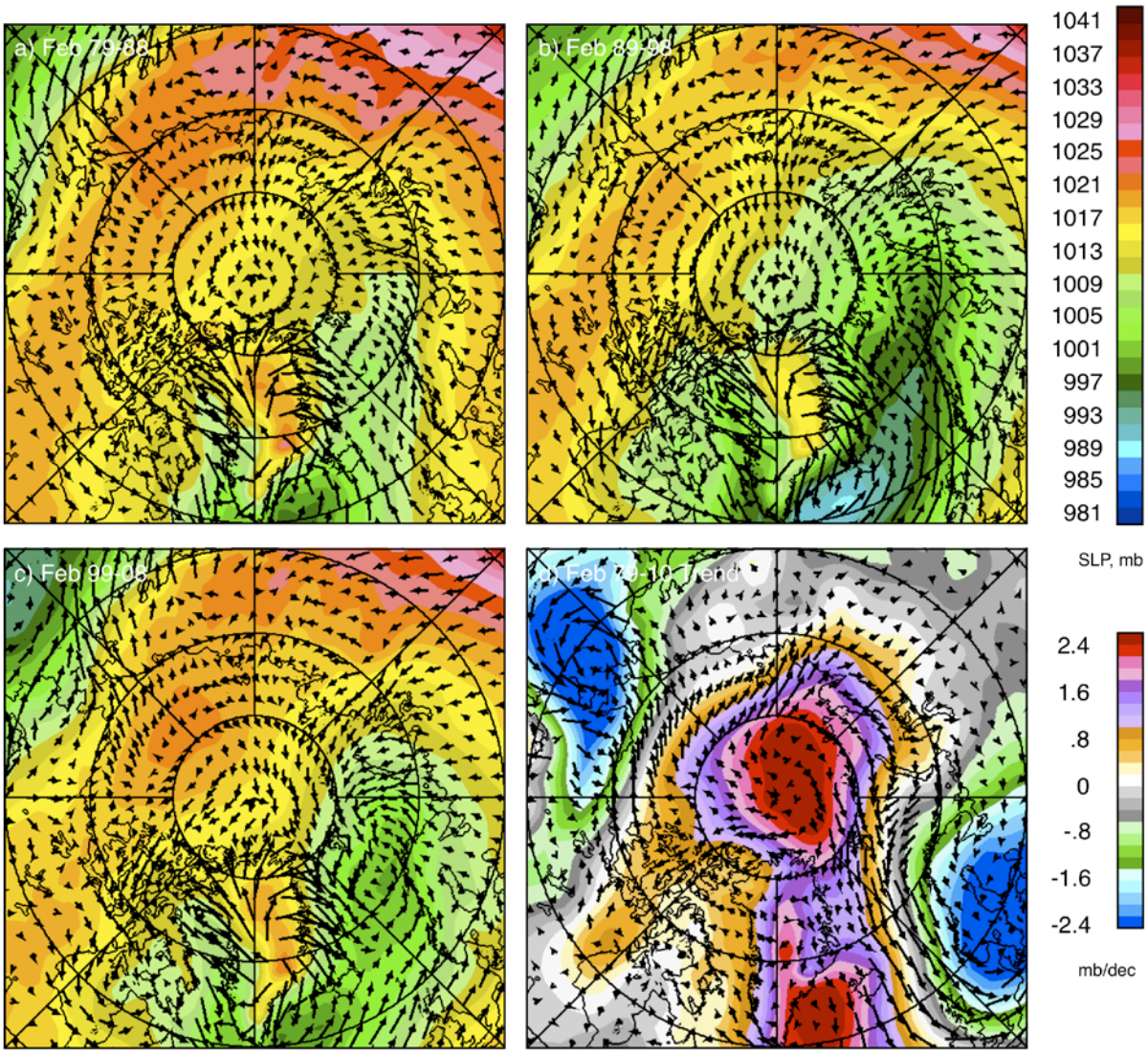

Figure 11. Multiyear averages of monthly SLP and winds in February for (a) 1979 to 1988; (b) 1989 to 1998; (c) 1999 to 2008; and (d) trends in sea level pressure and winds from 1979 to 2009

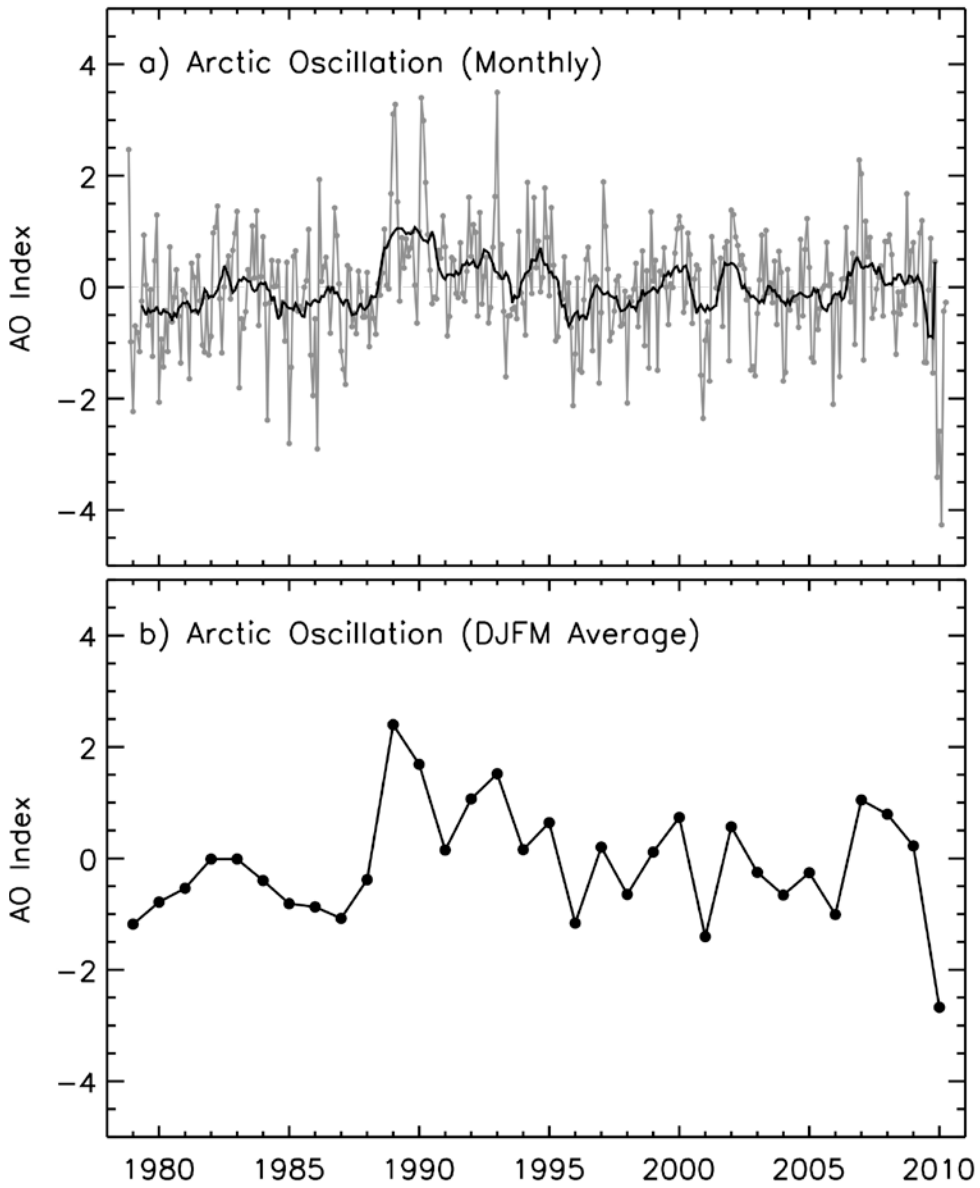

Figure 12. Arctic Oscillation indices (a) for each month from November 1978 to December 2010; and (b) for each winter (DJFM) from 1979 to 2010.